Characterization of Measurement Uncertainties in Crack Profiles Assessed by In-Line Inspection Tools

Smitha D. Koduru
Research Engineer, C-FER Technologies, Edmonton, Canada

Dongliang Lu
Researcher, C-FER Technologies, Edmonton, Canada

Jason B. Skow
Department Manager, C-FER Technologies, Edmonton, Canada

ABSTRACT: Measurement quantities representing crack profile geometric parameters are evaluated for their influence on the failure pressure of pipelines. Several representative cases of pipe designs are considered to isolate the influence of geometric parameters from that of pipe parameters such as pipe size, grade, wall thickness, and toughness. The results indicate the ratio of crack profile area to the crack length as the most influential geometric quantity. Using this measurement quantity, it becomes straightforward to evaluate the reliability of the ILI measurements for crack profiles and quantify the associated measurement uncertainties with probabilistic measures.

1. INTRODUCTION

The primary objective of this study is to identify measurement quantities that reliably characterize the uncertainties associated with crack profile measurements made using in-line inspection (ILI) tools. The secondary objective of this study is to establish a methodology that evaluates the suitability of these quantities to represent measurement uncertainty in ILI tools from the perspective of pipeline pressure capacity.

ILI tools are commonly used to identify and size defects in buried pipelines. With increasing number of ILI inspections and the associated in-ditch field measurement of defects, a reliable estimate of ILI measurement error is possible (Skow and LeBlanc 2014). The uncertainty associated with the defect detection, the correct identification of defect type, and sizing, are characterized by probabilistic measures such as, Probability of Detection (PoD), Probability of Identification (PoI), confidence interval on the defect depth sizing, and length sizing (API 2013, Lu et al. 2014). These measures of uncertainty are necessary inputs to quantitative pipeline risk assessments, which result in an increased consistency in risk management across the pipeline system.

Assessing pipeline pressure capacity using the ILI length and the maximum depth measurements results in an inconsistent risk estimation. For example, a crack with a long shallow region in the profile that is unlikely to result in pipe rupture (Fessler and Rapp 2014) could be categorized as a critical crack. Therefore, the shape of crack cross-section profile has a significant influence on assessing pressure capacity. Measurement uncertainties in length and maximum depth are inadequate to account for the influence of variability in crack shape. This necessitates the development of probabilistic measures that explicitly account for the measurement uncertainties in crack profile shape.

A crack profile is a series of depth measurements corresponding to a number of locations along the axial length of a crack on the pipe's exterior. A typical field-measured crack profile is shown as the dotted line in Figure 1. The depth measurement method depends on the field

procedures adopted, which includes ultrasonic tools (UT), magnetic particle inspection, and surface grinding with UT depth measurements at specific intervals. Depending on the field procedures, the available crack profile values for depth are measured at either fixed length intervals or variable intervals.

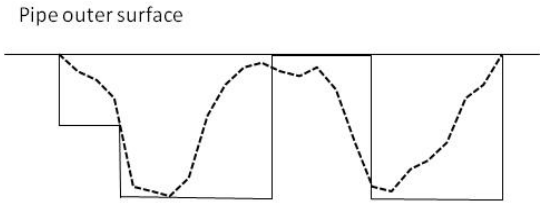

Figure 1: Crack profile measured by ILI and field techniques

Characterizing the measurement error associated with a crack profile is different than for length and depth sizing. As seen in Figure 1, the difference between the ILI measurements (solid line), and field measurements (dotted line) may be independent of total length and maximum depth sizing. In this example, the maximum depth and length of both measurements are equal. However, there is clearly a discrepancy in the profile shape.

Another difficulty in the comparison of field and ILI profiles is determining the method to superimpose them. This difficulty arises due to the lack of a common reference location for both measurements. One option is the use of crack maximum depth to align profiles. However, there is a significant uncertainty in the axial location of maximum crack depth. ILI measurements of crack profile are too coarse to accurately provide the location of maximum depth of a crack. As a result, it is difficult to assess portions of a profile that are missed by the ILI measurement and if the missing portions are significant for burst pressure assessment.

Sizing parameters such as length, maximum depth and area, may not distinguish critical crack profiles. Due to the presence of large shallow portions in cracks and due to the discrepancy in the measurement methods, the ILI length sizing may appear to have a large error (Skow and LeBlanc 2014). Furthermore, the measurement errors in maximum depth and length may have a smaller influence on the pressure capacity than the shape of the crack profile. As a result, expressing measurement error as a function of these parameters may skew the risk assessment results.

The following sections describe the scope, the measurement quantities, and a methodology for the selection of the optimal measurement quantity. Finally, conclusions and potential future work are discussed.

2. SCOPE

The scope is limited to the probabilistic analysis of the selected measurement quantities to assess their influence on the pipe burst pressure. The measurement quantities proposed for assessing the reliability of ILI profile measurements are:

1. Maximum crack depth (d)
2. Surface length (l)
3. Crack perimeter excluding surface length (p)
4. Crack section area (a)
5. Aspect ratio (d/l)
6. Area to length ratio (a/l)
7. Area to perimeter ratio (a/p)
8. Area to depth ratio (a/d)

Each quantity in the above list is selected from basic profile geometry such as d, l, a, and combinations of these measures. Note that the pipe attributes, such as wall thickness, toughness, and so on, are not used so that the measurement error remains independent of these attributes. Since experimental data for the pipe failure pressures and corresponding crack profile measurements is limited, the CorLAS® model by Jaske and Beavers (2001) is selected for the computation of predicted burst pressure (PBP) of a pipe.

In the CorLAS® model, burst pressures are calculated by considering portions of crack profiles with varying crack lengths. For example, the crack profile shown in Figure 2 is evaluated for all the lengths L_i, where i = 1, 2, 3, 4. These evaluations are repeated at each length coordinate l_i. The minimum burst pressure computed among

all the portions of a crack profile is the PBP. Thus, the model evaluates the most influential portion of a crack profile. It is shown to have the lowest variability in the PBP to the input parameter assumptions (Polasik et al. 2014), and the best predictive capability in comparison with limited experimental data (Tandon et al. 2014).

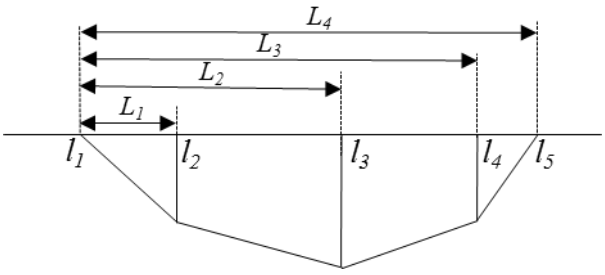

Figure 2: Portions of a crack profile evaluated using the CorLAS® model

Note that the results of the present study are likely a representation of the sensitivity of the CorLAS® model to the listed measurement quantities rather than true representation of the influence on burst pressure. However, as the CorLAS® model is extensively employed in the pipeline industry, the results of this study are useful for a rapid assessment of the ILI measurement reliability that is consistent with PBP estimates. Using the results of present study, this becomes possible without a particular consideration for remaining pipeline characteristics, such as pipe grade, NPS, thickness, and toughness.

3. METHODOLOGY

A set of pipes based on the case matrix for nominal pipe size (NPS) with varying maximum allowable operating pressure (MAOP), and specified minimum yield strength (SMYS) are shown in Table 1. These combinations are based on viable designs according to CSA Z662 (2011), ASME B31.8 (2014) and ASME B31.4 (2012) for class location 1 to 4. A total 128 sample pipes with a wide range of combinations for operating pressure, size, pipe wall thickness (*t*), and pipe grades are considered.

Table 1: Pipe sizes (NPS) for the matrix of cases

MAOP	*SMYS (MPa)*				
(MPa)	*241*	*290*	*359*	*448*	*550*
4.48	*12,30*	*20,48*	*30,48*	-	-
5.86	*8,12*	*12,20*	*20,30,48*	*30,48*	-
7.93	*8*	*8,12*	*8,20*	*12,30*	*48*
10.00	-	*8*	*8,12*	*8,20*	-
12.07	-	-	*8*	*8,12*	-
15.17	-	-	-	*8*	-

For all sample cases, the parameters listed in Table 2 are represented by random variables. In order to represent a wide range of crack profile types, crack depths are chosen to have the maximum variation physically possible. Due to the physical process of crack growth, adjacent crack depth coordinates are likely correlated. However, in the absence of the correlations required for modeling such spatial variation, the series of depth values within a profile are assumed to be uncorrelated. For crack length, the distribution is estimated from a combination of prior experience and the values presented in Fesseler and Rapp (2014). CVN values are known to have large variations for pipe grades with low SMYS compared to higher grades. Therefore, the upper bound and lower bound values of CVN corresponding to each pipe grade are selected separately, as shown in Table 3.

Table 2: Random variable parameters

Random Variable	*Distribution*	*Mean*	*Coefficient of Variation*
CVN[1]	*Uniform*	*Varies*	*0.57*
Length	*Lognormal*	*178 mm*	*1.75*
Depth[2]	*Uniform*	*t/2*	*0.57*

[1]Charpy V-notch Number
[2]Lower bound = zero; Upper bound = *t*

For each case, 50,000 simulated crack profiles were generated. The simulation procedure for crack profiles is as follows:

- Generate random realization for crack length following the distribution in Table 2
- Divide each realization of crack length in to 12.7 mm (equal to half-inch) intervals resulting in n_d number of length coordinates
- Generate n_d random realizations of crack depths associated with length coordinates for each simulated crack length

Table 3: Distribution parameters for CVN

SMYS (MPa)	*Lower Bound (J)*	*Upper Bound (J)*
241	*6.78*	*67.78*
290	*6.78*	*135.58*
359	*6.78*	*135.58*
448	*27.12*	*135.58*
550	*27.12*	*135.58*

From the above procedure, simulated crack profiles result in a set of length and depth coordinates similar to field measurements. The crack profile measurements and the associated random realizations of CVN are then employed to compute PBP. In addition to PBP, "equivalent length" and "equivalent depth", which are the length and depth of a semi-elliptical crack with equivalent PBP, are also computed as a by-product of the CorLAS® method. Furthermore, for each realization of a crack profile, the proposed measurement quantities noted in Section 2 are also computed.

Figure 3 shows a sample realization of crack profile simulated with the above procedure represented with a solid line. The dotted rectangle represents the assumptions regarding crack profile based on maximum depth and length of the crack, while the grey semi-ellipse represents the "equivalent" crack with same PBP as the simulated crack profile computed using the CorLAS® method. The pipe parameters are listed in the gray labels above and to the right of the figure.

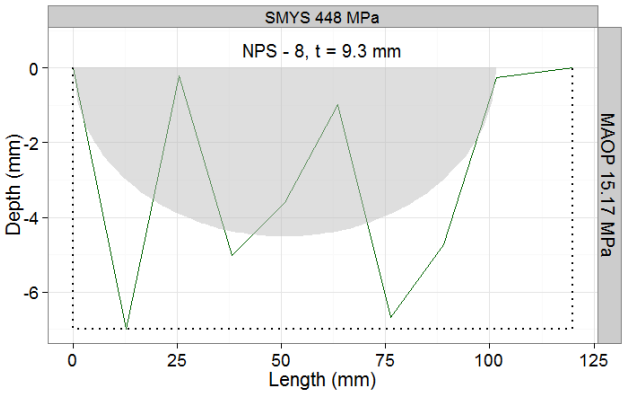

Figure 3: Sample simulated crack profile

Following the simulation procedure, the conditional expectation of PBP for each measurement quantity and for each pipe case is computed. The computation procedure is as follows:

- Divide each quantity in to a set of bins with unit intervals
- If the number of bins from the above step are less than ten, decrease the bin interval to have a minimum of ten bins
- Sort PBP values in to corresponding bins
- Compute conditional expectation of PBP for each bin
- Compute variance of the conditional expectation of PBP

A sample calculation from the above procedure is shown in Table 4 for measurement quantity, *a/p* for the pipe case corresponding to parameters shown in Figure 3. The conditional expectation of PBP decreases with increasing *a/p*. This is predictable since the increase in *a/p* reflects increase in crack size and therefore, causes a decrease in expected pipe failure pressure. Furthermore, Table 4 shows sufficient sample size in each bin to compute the expected value, and sufficient number of bins to compute the variance of expectation. As all the parameters considered had similar sample sizes, initial sample size of 50,000 considered for simulated crack profiles for each case in Table 1 is deemed sufficient. In addition to the variance of the conditional expectation, the total variance of PBP

is computed. The difference in total variance and the variance of the conditional expectation represents the error for the overall predictor of PBP, as follows:

$$e_i = Var(PBP) - Var(E[PBP|\delta_i]) \quad (1)$$

where e_i is the error corresponding to the measurement quantity, δ_i considered. The variance of the conditional expectation of PBP represents the variance in PBP that is caused due to the variability in the measurement quantity, δ_i. Therefore, the error, e_i denotes the variance of PBP that is unexplained by variability in δ_i, and the influence of all other measurement quantities other than δ_i on the variance of PBP. Hence, the measurement quantity that corresponds to minimum error is the best overall predictor for PBP.

Table 4: Conditional expectation of PBP for a/p

a/p (mm)		*Sample Size*	*E[PBP|(a/p)] (MPa)*
Bin lower bound	*Bin upper bound*		
0.00	*0.67*	*827*	*43.64*
0.67	*1.35*	*1287*	*42.90*
1.35	*2.02*	*2260*	*41.52*
2.02	*2.69*	*4231*	*39.05*
2.69	*3.37*	*7685*	*35.06*
3.37	*4.04*	*12520*	*29.22*
4.04	*4.71*	*13377*	*22.47*
4.71	*5.39*	*4599*	*19.68*
5.39	*6.06*	*695*	*16.68*
6.06	*6.73*	*37*	*13.53*

Table 5 shows the error corresponding to each measurement quantity for the pipe case and parameters shown in Figure 3. The measurement quantity, *a/l* has the absolute minimum error for this case.

In order to compare the error between all the pipe cases considered, the error computed according to Eq.(1) is normalized by the total variance of PBP for each pipe case. Furthermore, normalized error, e_n, in PBP is also estimated for equivalent depth, and equivalent length. These results are discussed in the following section.

Table 5: Error of PBP for overall prediction δ_i

δ_i	e_i
d	*21.06*
l	*40.87*
p	*40.78*
a	*42.43*
d/l	*23.07*
a/l	*-17.63*
a/p	*-23.96*
a/d	*42.89*

4. RESULTS AND DISCUSSION

Figure 4 shows the e_n plotted for each pipe case for all the measurement quantities listed in Section 2. Three clusters of error are observed with *l*, *p*, *a*, and *a/d* in one cluster showing largest errors, *d*, and *d/l* in the second cluster with a low positive error, and a third cluster with *a/l* and *a/p* with a low negative error. From Figure 4, it is evident that *d* (light green line), and *a/l* (dark blue line) have minimum absolute error among all the measurement quantities. Therefore, these two quantities are considered for further inspection.

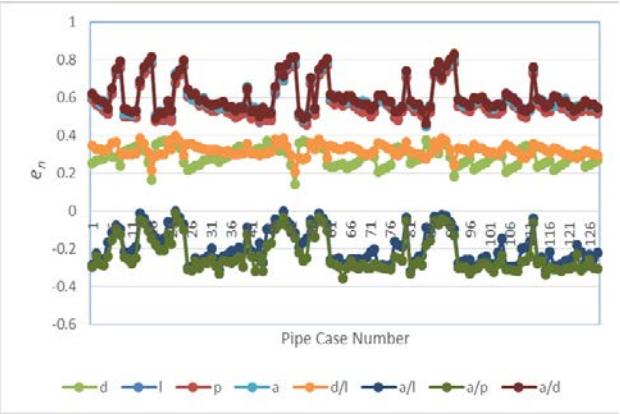

Figure 4: Comparison of e_n for all measurement quantities for each case

Of the 128 pipe cases, 92 cases have *a/l* as the best overall predictor for PBP. The remaining 36 cases have *d* as the best overall predictor for PBP. Table 6 shows the pipes with *d* as the best

overall predictor for PBP. A majority of pipes among the 36 cases have NPS 8 and class 1 design. A comparison of absolute e_n between *d* and *a/l* in Figure 5 for these 36 cases indicates that the difference in error between these two quantities is less than 10% on average.

Table 6: Pipe cases with d as the best overall predictor for PBP

NPS	*SMYS (MPa)*	*MAOP (MPa)*	*Class*
8	*241*	*5.86*	*1-4*
8	*241*	*7.93*	*1-4*
8	*290*	*7.93*	*1-3*
8	*290*	*10.00*	*1-2*
8	*359*	*7.93*	*1-4*
8	*359*	*10.00*	*1-3*
8	*359*	*12.07*	*1,3*
8	*448*	*10.00*	*1-4*
8	*448*	*12.07*	*1-4*
8	*448*	*15.17*	*1*
12	*241*	*4.48*	*1*
12	*290*	*5.86*	*1*
12	*359*	*10.00*	*1*
12	*448*	*7.93*	*1-2*

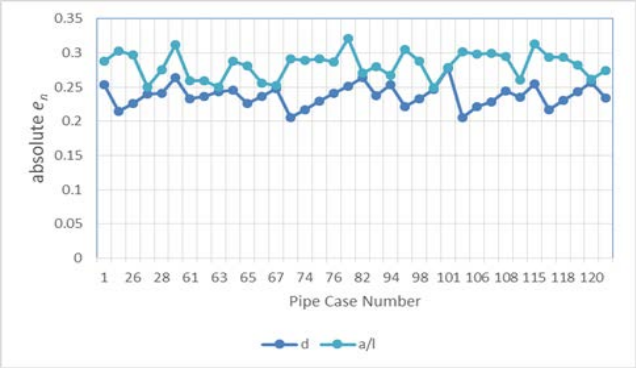

Figure 5: Comparison of e_n between d and a/l for pipe cases with minimum e_n for d

From the above analysis, *a/l* is recommended as the best geometric measurement quantity to be considered to assess measurement errors in crack profiles.

Figure 6 shows the comparison of e_n of *d* and *a/l* with the equivalent depth. For all the pipe cases considered, the equivalent depth has the minimum absolute e_n and is the best overall predictor for PBP, which is as anticipated from the CorLAS® method. Note that equivalent depth is not available from crack geometry alone and therefore, it is not considered in the measurement quantities list in Section 2. Measurement quantity *a/l* has similar e_n as equivalent depth for a majority of pipe cases. Only seven pipe cases have e_n of *d* closer to e_n of equivalent depth. All other cases have e_n of *a/l* closer to e_n of equivalent depth. These seven pipe cases are thin-walled pipes with wall thickness less than 4.5mm, as shown in Table 7.

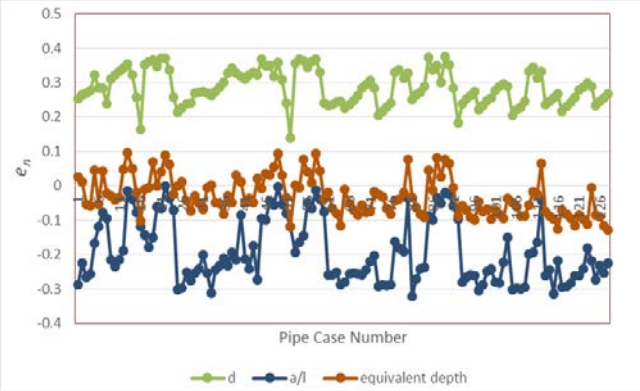

Figure 6: Comparison of e_n for d, a/l, and equivalent depth for each pipe case

Table 7: Pipe cases with normalized error of d closer to equivalent depth in comparison with a/l

NPS	*SMYS (MPa)*	*t (mm)*
8	*241*	*3.7*
8	*241*	*4.4*
8	*290*	*4.2*
8	*359*	*3.4*
8	*359*	*4*
12	*241*	*4.2*
12	*290*	*4.5*

This study considered relatively long features with a mean crack lengths of 178mm. Therefore, the influence of short and deep cracks may be underestimated. However, the application of the methodology presented here to a data set with field measured crack profiles would improve the

confidence in the preliminary results obtained from this study and is recommended for future work.

5. CONCLUSIONS

The ratio of crack profile area to the length is presented as the best overall predictor for PBP among the geometric measurement quantities considered. Furthermore, a methodology for assessing the best overall predictor from the crack profile data sets available from field measurements is presented. This assessment provides a method to quantify the measurement uncertainty in the crack profile shape allowing for the development of probabilistic measures for crack profile sizing accuracy of ILI tools. This is in contrast to the existing methods of characterizing the ILI measurement error based solely on the error in crack depth assessments. The proposed methodology provides an error measure that includes all the available information regarding a crack profile, such as length, depth, and profile shape.

In future work, this methodology must be applied to validate the proposed measurement quantity using data sets of field crack profile measurements and ILI measurements. Applying the proposed methodology and validating the measurement quantities for the burst pressure predictions from other mathematical models, and experimental results is also recommended.

6. REFERENCES

API 1163 (2013), *In-line Inspection System Qualification*, American Petroleum Institute, Washington DC, U.S.A.

ASME B31.4 (2012), *Pipeline Transmission Systems for Liquid Hydrocarbons and Other Liquids*, American Society of Mechanical Engineers, New York, NY, U.S.A

ASME B31.8 (2014), *Gas Transmission and Distribution Piping Systems*, American Society of Mechanical Engineers, New York, NY, U.S.A

CSA Z662 (2011), *Oil and Gas Pipeline Systems. CSA Z662-2011*, Canadian Standards Association, Mississauga, ON, Canada

Fessler, R.R., and Rapp, S.C. (2014), "The effect of shallow cracks on the predicted failure pressure of natural gas pipelines containing stress-corrosion cracks", In *Proceedings of the ASME 2014 10th International Pipeline Conference, IPC 2014*, September 29 – October 3, 2014, Calgary, Alberta, Canada

Jaske, C.E., and Beavers, J.A., (2001), *Integrity and Remaining Life of Pipe with Stress Corrosion Cracking*, Final Report on PR 186-9709, Pipeline Research Council International, Inc., Arlington, VA.

Lu, D., Skow, J.B., and Keane, S. (2014), "Assessing the probability of detecting crack features using ultrasonic in-line inspection tool run results and excavation data", In *Proceedings of the ASME 2014 10th International Pipeline Conference, IPC 2014*, September 29 – October 3, 2014, Calgary, Alberta, Canada

Polasik, S.J., Keane, S., Harper, W.V., and Bubenik, T., (2014), "Quantifying the impact of assumptions on predicted burst pressure assessments", In *Proceedings of the ASME 2014 10th International Pipeline Conference, IPC 2014*, September 29 – October 3, 2014, Calgary, Alberta, Canada

Skow, J.B., and LeBlanc, L. (2014), "In-line inspection tool performance evaluation using field excavation data", In *Proceedings of the ASME 2014 10th International Pipeline Conference, IPC 2014*, September 29 – October 3, 2014, Calgary, Alberta, Canada

Tandon, S., Gao, M., Krishnamurthy, R., Kariyawasam, S., and Kania, R.,(2014), "Evaluation of existing fracture mechanics models for burst pressure predictions, theoretical and experimental aspects," In *Proceedings of the ASME 2014 10th International Pipeline Conference, IPC 2014*, September 29 – October 3, 2014, Calgary, Alberta, Canada